Carbon-13 Relaxation Behavior in Multiply Enriched Systems: [90%-1,2-$^{13}C_2$-Gly^6]Bradykinin†

R. E. London,* Martin Phillippi, and John Stewart

ABSTRACT: The relaxation behavior of macromolecules multiply enriched in ^{13}C has been investigated theoretically, and results for [90%-1,2-$^{13}C_2$-Gly^6]bradykinin have been interpreted on the basis of this theory. The ^{13}C–^{13}C dipolar interaction can be selectively observed by comparing the relaxation behavior of the singly labeled (center) and doubly labeled satellite ^{13}C resonances, and the results can be used to evaluate the rotational correlation time of carbon–carbon bonds. In both the present study and all of the multiple labeling studies reported to date, the rotational correlation times thus obtained (τ_{CC}) are significantly longer than the rotational correlation times (τ_{CH}) obtained in the usual way on the basis of relaxation analysis of protonated carbons. The spin–lattice relaxation behavior for doubly ^{13}C labeled systems falls into three limits: (1) extreme narrowing limit in which the ^{13}C–^1H and ^{13}C–^{13}C dipolar interactions are additive; (2) spin-diffusion limit in which the relaxation rate is limited by the rate of ^{13}C–^{13}C flip-flop interactions leading to spin diffusion; (3) spin-diffusion limit in which the rate is determined by the protonated carbon which becomes a relaxation sink. In addition to the spin–lattice relaxation differences between singly and multiply labeled molecules, significant line-width differences are also observed. These do not reflect ^{13}C–^{13}C dipolar broadening but rather the incipient collapse of the doublet structure due to the short T_1 of the scalar coupled carbon. In the case of [90%-1,2-$^{13}C_2$-Gly^6]bradykinin, the carbonyl doublet is broadened relative to the center resonance due to the short Gly methylene T_1. This effect is analogous to the collapse of the multiplet structure of spin $^1/_2$ nuclei bonded to quadrupolar nuclei. The resulting spectrum can be analyzed quantitatively to obtain the Gly methylene T_1. The method therefore provides a quick (single spectrum) means for obtaining T_1 information which may otherwise be difficult to obtain due to broadening or overlap of resonances. Studies of the labeled bradykinin have been carried out in solvents of varying viscosity and the data analyzed by using the theory presented. At very high viscosities, overall molecular motion is greatly reduced, and the effects of internal segmental motion become unmasked. Therefore, the relaxation behavior of peptides in high viscosities is found to differ from that of globular proteins for which segmental motion is estimated to be of lower amplitude and consequently less significant as a relaxation mechanism.

^{13}C spin–lattice relaxation measurements provide a powerful tool for the study of solution dynamics of complex biologically interesting molecules [London (1980) and references cited therein]. Allerhand (1978) and co-workers have made pioneering measurements on unlabeled proteins; however, more recently, extensive use has been made of isotopic enrichment with the dual object of spectral simplification and sensitivity enhancement leading to time reduction for the lengthy relaxation measurements. Enrichment of adjacent nuclei has generally been avoided due to the increased complexity resulting from scalar ^{13}C–^{13}C spin–spin coupling interactions; however, in appropriately chosen systems, the ^{13}C–^{13}C dipolar interaction may provide useful dynamic information. Enrichment at levels below 100% leads to the presence of isotopic isomers corresponding to both the multiply enriched and the singly enriched compounds. Simultaneous T_1 measurements can then be performed and the ^{13}C–^{13}C dipolar interaction evaluated specifically by subtraction, thus solving the problem of determining the relaxation mechanism. An additional motivation for this approach is the uncertainty in the C–H bond lengths, which can lead to relatively large errors in calculated rotational correlation times in some cases (Dill & Allerhand, 1979). Such uncertainties are expected to be considerably less significant for carbon–carbon bonds.

In addition to the spin–lattice relaxation differences between the ^{13}C center and satellite resonances, line-width differences can also be observed in some cases. This effect is related to the short T_1 of the directly bonded carbon. Broadening and eventual collapse of the multiplet structure for spin $^1/_2$ nuclei bonded to nuclei with short T_1 values were, in fact, first considered for a system of two spin $^1/_2$ nuclei (Gutowsky et al., 1953); however, the effect is most commonly observed if the second nucleus is quadrupolar (Pople, 1958). As a result of the relatively slow tumbling of large biological molecules, T_1 values for protonated ^{13}C nuclei can be sufficiently short to produce this effect in directly bonded spin $^1/_2$ nuclei. The effect can be used to obtain T_1 information from a single spectrum and, as in the present case, is applicable to systems in which the protonated nucleus may be too broad to permit direct observation. The approach is limited by the fact that for slowly tumbling molecules, ^{13}C–^{13}C dipolar broadening may also become significant.

The present study of [90%-1,2-$^{13}C_2$-Gly^6]bradykinin in glycerol/water mixtures of varying viscosity was undertaken in order to evaluate the use of multiple ^{13}C labeling as a dynamic probe of biological macromolecules.

Materials and Methods

[90%-1,2-$^{13}C_2$-Gly^6]Bradykinin was synthesized and characterized similarly to [20%-1,2-$^{13}C_2$-Gly^6]bradykinin described previously (London et al., 1979). Glycerol-d_8 was obtained from Merck. For the studies at high glycerol/D_2O ratios, the aqueous sample was evaporated to dryness and redissolved in the glycerol. Small aliquots of D_2O were then added subsequently in order to achieve high viscosities without significant sample dilution.

NMR measurements were carried out on either a JEOL FX90Q (ν_C = 22.63 MHz) (for the measurements of the

† From the Los Alamos National Laboratory, University of California, Los Alamos, New Mexico 87545 (R.E.L. and M.P.), and the University of Colorado Medical Center, Denver, Colorado 80220 (J.S.). *Received June 2, 1981; revised manuscript received September 16, 1981.* This work was performed under the auspices of the U.S. Department of Energy.

0006-2960/82/0421-0470$01.25/0

peptide in D_2O only) or a Varian XL-100-15 NMR spectrometer (ν_C = 25.14 MHz) interfaced to a Data General Supernova computer for Fourier-transform operation. Thus, only the measurements on the peptide which corresponded to the motion in the extreme narrowing limit were carried out on the 22.63-MHz instrument so that the small frequency difference does not affect the results.

Spin–lattice relaxation measurements were made by using either an inversion–recovery sequence or, in the case of peptide in pure glycerol-d_8, the variable nutation angle approach described by Gupta (1977). In the former case, the 90° observation pulse will lead to mixing of the intensities within a given multiplet only due to the weakly coupled AX nuclei (Schaublin et al., 1974). For a 90° observation pulse, no differences were observed in the recovery rates of the two doublet resonances, as expected. Measurements of the carbonyl T_1 values shortly after dissolving the peptide in D_2O and subsequently after a period of several months indicated that the T_1 values had decreased significantly, presumably due to leaching of paramagnetic ions from the NMR tube. It was concluded that treatment with Chelex might not be advisable due to binding of the positively charged peptide (which contains two arginine residues) to the resin. Instead, the sample was vigorously shaken with insoluble tetraphenylporphyrin (TPP) for a period of approximately 1 h and then filtered in the expectation that the latter could effectively remove some of the paramagnetic contaminants. This procedure appeared to be successful as the T_1 values increased by more than a factor of two. However, attempts to apply this procedure to a test sample with a 1 mM contamination of copper ions failed, perhaps due to the slow kinetics of the chelation. It is concluded that this procedure may be useful for treating very low levels of paramagnetic contamination of biological samples, and the efficiency might be further increased by heating.

Theory

The importance of ^{13}C–^{13}C dipolar interactions was first pointed out by Moreland & Carroll (1974). London et al. (1975a,b) used the extended Solomon equation framework for treating three interacting spins under conditions of complete proton decoupling. The discussion given was limited to the extreme narrowing region, and the behavior in the absence of this assumption is considered below. The coupled Solomon equations can be written

$$\frac{dA_z}{dt} = -g_A(A_z - A_0) - f_{AM}(M_z - M_0) + f_{AX}X_0 \quad (1a)$$

$$\frac{dM_z}{dt} = -g_M(M_z - M_0) - f_{AM}(A_z - A_0) + f_{MX}X_0 \quad (1b)$$

where the spins A, M, and X correspond to an unprotonated carbon, a directly bonded carbon, and the proton(s) bonded to M, respectively. The relaxation rate coefficients are given by

$$g_A = \frac{\gamma_c^2\hbar^2}{10}\sum_i \frac{N_i\gamma_i^2}{r_{ai}^6}\left[\frac{\tau}{1 + (\omega_A - \omega_i)^2\tau^2} + \frac{3\tau}{1 + \omega_A^2\tau^2} + \frac{6\tau}{1 + (\omega_A + \omega_i)^2\tau^2}\right] \quad (2)$$

$$f_{AM} = \frac{\gamma_A^2\gamma_M^2\hbar^2}{10r_{AM}^6}\left[\frac{-\tau}{1 + (\omega_A - \omega_M)^2\tau^2} + \frac{6\tau}{1 + (\omega_A + \omega_M)^2\tau^2}\right] \quad (3)$$

Analogous expressions can be written for g_M, f_{AX}, and f_{MX}. The nuclear Overhauser enhancements for the A and M spins are readily obtained from the solution of the following steady-state equations:

$$NOE_A = 1 + \left(\frac{g_M f_{AX} - f_{AM}f_{MX}}{g_A g_M - f_{AM}^2}\right)\frac{\gamma_H}{\gamma_C} \quad (4)$$

$$NOE_M = 1 + \left(\frac{g_A f_{MX} - f_{AM}f_{AX}}{g_A g_M - f_{AM}^2}\right)\frac{\gamma_H}{\gamma_C} \quad (5)$$

The relaxation behavior of the system is a sum of two exponentials

$$A_z(t) = A_{eq} + C_1'e^{-\lambda_1 t} + C_2'e^{-\lambda_2 t} \quad (6)$$

where

$$\lambda_{1,2} = g_A + g_M \pm \frac{[(g_A - g_M)^2 + 4f_{AM}^2]^{1/2}}{2} \quad (7)$$

and the coefficients are given by

$$C_1' = \frac{1}{\lambda_1 - \lambda_2}\left[\left(\frac{g_M f_{AX} - f_{AM}f_{MX} - \lambda_1 f_{AX}}{\lambda_1}\right)X_0 + [A_z(0) - A_0](\lambda_1 - g_M) + [M_z(0) - M_0]f_{AM}\right] \quad (8a)$$

$$C_2' = \frac{1}{\lambda_2 - \lambda_1}\left[\left(\frac{g_M f_{AX} - f_{AM}f_{MX} - \lambda_2 f_{AX}}{\lambda_2}\right)X_0 + [A_z(0) - A_0](\lambda_2 - g_M) + [M_z(0) - M_0]f_{AM}\right] \quad (8b)$$

where $A_0 = M_0 = \gamma_C H_0$, $X_0 = \gamma_H H_0$, $A_{eq} = A_0 NOE_A$, and $M_{eq} = M_0 NOE_M$. For an inversion–recovery experiment (Vold et al., 1972), we have

$$\frac{A_{eq} - A_z(t)}{2A_{eq}} = C_1e^{-\lambda_1 t} + C_2e^{-\lambda_2 t} \quad (9)$$

and setting $A_z(0) = -A_0NOE_A$, $M_z(0) = -M_0NOE_M$ gives

$$C_1 = \frac{-C_1'}{2A_{eq}} = \frac{1}{2(\lambda_2 - \lambda_1)NOE_A}\left[\left(\frac{g_M f_{AX} - f_{AM}f_{MX} - \lambda_1 f_{AX}}{\lambda_1}\right)\frac{\gamma_H}{\gamma_C} + (g_M - \lambda_1)(NOE_A + 1) - f_{AM}(NOE_M + 1)\right] \quad (10a)$$

$$C_2 = \frac{-C_2'}{2A_{eq}} = \frac{1}{2(\lambda_1 - \lambda_2)NOE_A}\left[\left(\frac{g_M f_{AX} - f_{AM}f_{MX} - \lambda_2 f_{AX}}{\lambda_2}\right)\frac{\gamma_H}{\gamma_C} + (g_M - \lambda_2)(NOE_A + 1) - f_{AM}(NOE_M + 1)\right] \quad (10b)$$

Analogous results can be obtained for $M_z(t)$ by interchanging M and A.

The behavior of the A and M magnetizations as a function of correlation time is illustrated in Figure 1. The T_1^{CH} values corresponding to the two values of r_{CH} indicated in the figure correspond to the usual relaxation behavior determined by the ^{13}C–^1H dipolar interaction (Allerhand et al., 1971). A corresponding T_1^{CC} curve using r_{CC} = 1.53 Å is also given, based

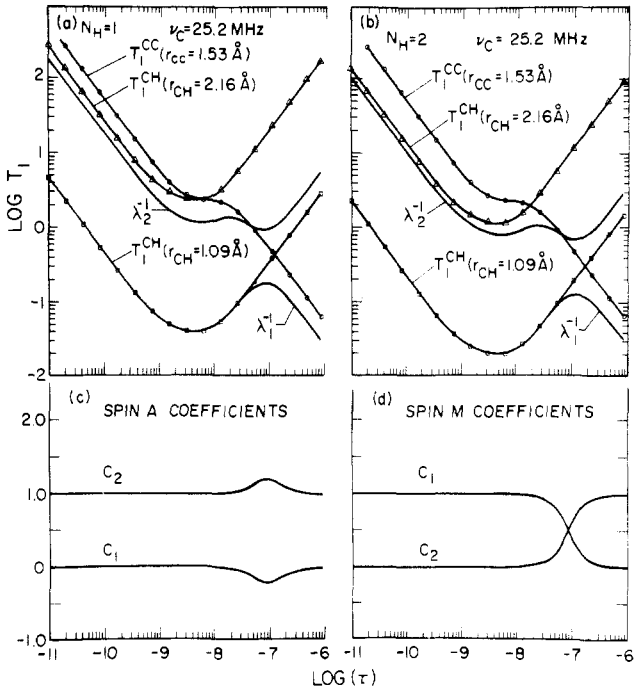

FIGURE 1: Spin–lattice relaxation behavior for an AM{X_n} system where A corresponds to a nonprotonated carbon for which r_{CH} = 2.16 Å, M corresponds to a protonated carbon with r_{CH} = 1.09 Å, and the proton(s) X is (are) decoupled. (a) T_1 behavior for A (△) and M (□) carbons in the absence of dipolar carbon–carbon interaction, the T_1 contribution corresponding to the carbon–carbon dipolar interaction with r_{CC} = 1.53 Å (eq 2) (○) and the two reciprocal eigenvalues λ_1^{-1} and λ_2^{-1} describing the relaxation of the A and M spins in the cross-relaxing system. Isotropic motion with rotational correlation time indicated on the abscissa is assumed. For long correlation times, the carbon–carbon term, g_A, becomes equal in magnitude to the carbon–carbon cross-relaxation term f_{AM}. (b) Same calculation but assuming N_H = 2 (i.e., two protons directly bonded to M), hence corresponding to the theoretical behavior of the labeled glycine. (c) Coefficients C_1 and C_2 corresponding to the eigenvalues λ_1 and λ_2 plotted in (a) as a function of the rotational correlation time. As can be seen from the curve, the spin–lattice relaxation behavior is effectively exponential over most of the range of correlation times considered and corresponds to the eigenvalue λ_2. (d) Coefficients corresponding to the eigenvalues λ_1 and λ_2 for the M relaxation. As a result of the crossover near $\tau = 10^{-7}$ s, the relaxation behavior is transferred from the λ_1 to the λ_2 curve for very slow motion.

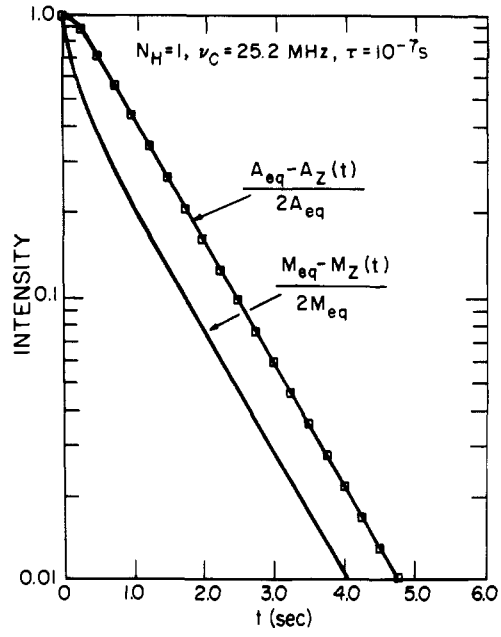

FIGURE 2: Behavior of the A and M magnetizations in an inversion–recovery experiment corresponding to a rotational correlation time $\tau = 10^{-7}$ s. The concave-downward A relaxation curve reflects mathematically coefficients which are greater than 1 and negative, as depicted in Figure 1c.

on eq 2. This curve would apply if one of the two interacting carbons is saturated and the other is observed. However, this is not generally the experimental procedure followed, and further, it may become impossible to effectively saturate one of the carbon resonances as it broadens, corresponding to longer rotational correlation times. However, to the extent that this approach is experimentally feasible, the ^{13}C–^{13}C dipolar interaction can become the dominant relaxation mechanism in macromolecules.

In the more usual experiment in which a nonselective pulse is applied to the ^{13}C spectrum, the relaxation behavior will be biexponential as described by eq 9 and 10a,b (Figure 1c,d). For the (nonprotonated) A spin, it can bee seen from Figure 1c that the relaxation is exponential down to correlation times of $\sim 10^{-8}$ s but becomes significantly nonexponental near $\tau = 10^{-7}$ s. The negative coefficient C_1 leads to a curve which is concave downward, as illustrated in Figure 2. In general, the relaxation behavior is determined primarily by λ_2. Three regions can be distinguished. In region I ($\tau \lesssim 10^{-8}$ s), the observed decay rate λ_2 is a sum of the ^{13}C–^{1}H and ^{13}C–^{13}C rates, as discussed in the literature. In region II (10^{-8} s $< \tau < 10^{-7}$ s), the cross-relaxation term f_{AM} becomes important, leading to a rate determined by spin diffusion; the f_{AM} cross-relaxation term is rate limiting. The relaxation sink in this case corresponds to the protonated M spin. In region III ($\tau > 10^{-7}$ s), the cross-relaxation rate exceeds the rate determined by the M sink, and hence, the latter becomes rate limiting. In this limit, Figure 1c indicates that the relaxation behavior is again exponential. Both carbons A and M will then have the same spin–lattice relaxation rate.

For the M spin, the crossover of coefficients indicated in Figure 1d allows the rate to follow approximately the T_1^{CH} curve so that λ_1 describes the relaxation for $\tau < 10^{-7}$ s while λ_2 relaxation is dominant for $\tau > 10^{-7}$ s. However, the decay will be highly nonexponential near $\tau = 10^{-7}$ s (Figure 2). It is apparent that in contrast to the ^{13}C–^{14}N interaction (Norton & Allerhand, 1976), the exponential approximation fails significantly in some motional regions requiring full consideration of the biexponential decay. Such nonexponential relaxation behavior has recently been observed in a solid-state ^{13}C NMR study of unlabeled hexamethylethane (Virlet & Ghesquieres, 1980). In the absence of ^{13}C enrichment, the ^{13}C–^{13}C dipolar interaction will become significant for much slower motion, i.e., near $\tau \sim 1/(\omega_C - \omega_{C'})$. The origin of this effect is, however, equivalent to that discussed here.

Effects of the carbon–carbon dipolar interaction on the line width are relatively small, leading to an approximately 50% increase in the line width over that predicted for a single ^{13}C–^{1}H dipolar interaction at an internuclear distance of 2.16 Å. The effect of the ^{13}C–^{13}C dipolar interaction is relatively more important near 10^{-9} s due to the different inflection points in the contributions (Figure 3). For many correlation times of interest, this broadening is substantially below the typical field inhomogeneity contribution. However, a second line-broadening effect which is significant is considered below.

As has been noted previously (London et al., 1975a), the additional carbon–carbon dipolar interaction can significantly reduce the $^{13}C\{^1H\}$ nuclear Overhauser enhancement for nonprotonated carbons. NOE_A values as a function of the rotational correlation time τ are summarized in panels a and b of Figure 4, corresponding respectively to either one or two protons bonded to M. Although the predicted effects are

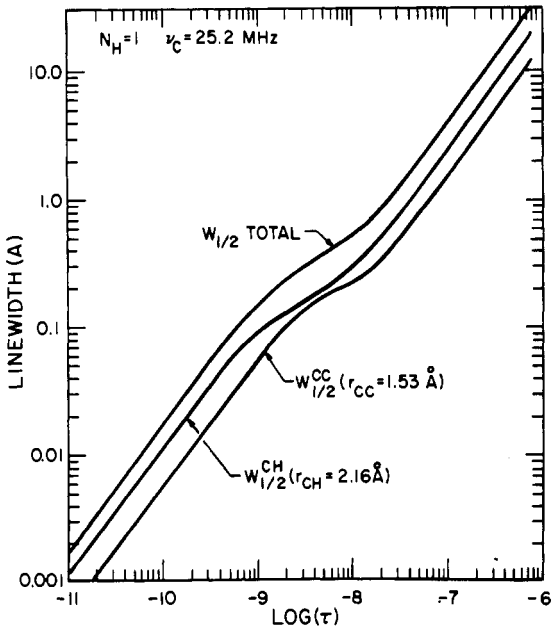

FIGURE 3: Dipolar line widths for the A (nonprotonated) carbon resonance. The contributions corresponding to a single proton with internuclear distance r_{CH} = 2.16 Å, to a single carbon with internuclear distance r_{CC} = 1.53 Å, and the total line-width contribution are given.

clearly significant, the additional relaxation contributions of longer range intramolecular ^{13}C–^{1}H dipolar interactions, intermolecular dipolar interactions for spin A, and other relaxation mechanisms such as ^{14}N–^{13}C dipolar interactions (Norton & Allerhand, 1976) and chemical shift anisotropy which may be significant for nonprotonated nuclei will reduce the magnitude of this effect (Figure 4c,d). Further, the shorter T_1 value for A resulting from the additional ^{13}C–^{13}C dipolar interaction will enhance the multiplets relative to the center resonance if the system is overpulsed. Nevertheless, these NOE effects can be significant in the interpretation of labeling probabilities resulting from ^{13}C enrichment.

Calculations including cross-correlation effects have recently been reported by Canet et al. (1979) for a C–C–H system. Significant perturbations can be predicted for the initial decay rates; however, such effects are of extremely short duration, essentially disappearing after $[A_{eq} - A_z(t)]/(2A_{eq})$ has decayed to 0.975. We have not observed such effects in the present experiments, reflecting in part the insufficient sensitivity required to obtain very accurate intensities corresponding to the initial decay as well as the fact that the present system is closer to AMX_2. Cross-correlation effects may be of greater significance near the T_1 minimum as found previously (London & Avitabile, 1976).

An interesting theoretical effect which, to the best of our knowledge, has not been discussed previously arises from the short T_1 of the methylene carbon (spin M). The short T_1 of the M spin can lead to multiplet collapse, analogous to the situation observed for protons bonded to quadrupolar nuclei such as ^{14}N:

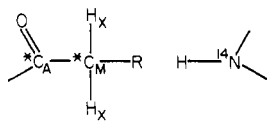

Calculation of the spectrum can be accomplished by using the A matrix as described by Abragam (1961):

$$\mathbf{A}_{m,m'} = \left[i(\omega_0 - \omega + Jm) - \frac{1}{\tau_m} \right] \delta_{m,m'} + P_{m,m'} \quad (11)$$

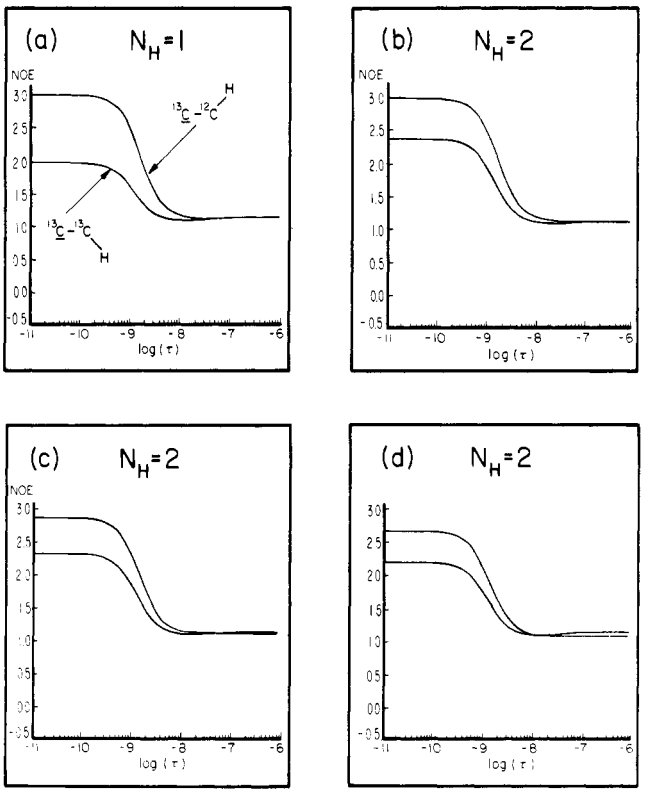

FIGURE 4: Nuclear Overhauser enhancements for the A (nonprotonated) carbon in the presence and absence of the additional carbon–carbon dipolar interaction corresponding to N_H = 1 (a) or N_H = 2 (b). In either case, the NOE_A = 3.0 in the extreme narrowing limit and in the absence of the ^{13}C–^{13}C dipolar interaction since no relaxation mechanism other than the ^{13}C–^{1}H dipolar mechanism is assumed. Effects of additional chemical shift anisotropy mechanism with $\Delta\sigma$ = 124 ppm (Jeffers et al., 1978) (c) and chemical shift anisotropy plus ^{14}N–^{13}C dipolar relaxation (d) are also illustrated for the N_H = 2 case.

where $P_{m,m'}$ is the transition probability per unit time from state m to m' and

$$\frac{1}{\tau_m} = \sum_{m'} P_{m,m'}$$

The relation of these transition probabilities to the T_1 value for spin M can be obtained from a consideration of the nuclear spin equilibrium. Letting n_+ and n_- represent the populations of the upper and lower states, we have

$$\frac{dn_+}{dt} = -P_{1/2,-1/2} n_+ + P_{-1/2,1/2} n_-$$

$$\frac{dn_-}{dt} = -P_{-1/2,1/2} n_- + P_{1/2,-1/2} n_+$$

Solving for the observable quantity $n_+ - n_-$ then gives

$$\frac{d}{dt}(n_+ - n_-) = 2P(n_+ - n_-)$$

where P is the mean of $P_{1/2,-1/2}$ and $P_{-1/2,1/2}$. Neglecting the differences between $P_{1/2,-1/2}$ and $P_{-1/2,1/2}$ as is done in the quadrupolar case (Pople, 1958) (high-temperature approximation) gives

$$P_{1/2,-1/2} = P_{-1/2,1/2} = \frac{1}{2T_1}$$

Thus, the A matrix becomes

$$\mathbf{A} = \begin{bmatrix} i(\omega_0 - \omega + \frac{1}{2}J) - \frac{1}{2T_1} & \frac{1}{2T_1} \\ \frac{1}{2T_1} & i(\omega_0 - \omega - \frac{1}{2}J) - \frac{1}{2T_1} \end{bmatrix} \quad (12)$$

Table I: Spin–Lattice Relaxation Times for [90%-1,2-$^{13}C_2$-Gly^6] Bradykinin

solvent	viscosity ratio[a]	T_1-(center) (s)	T_1-(satellites) (s)	T_1^{CC} (s)	τ_0[c] (s)
D_2O	1.0	2.6	2.2	14.3	3.9×10^{-10} 2.3×10^{-10} [b]
30% D_2O/70% glycerol-d_8	20	0.90	0.65	2.3	7.8×10^{-9}
10% D_2O/90% glycerol-d_8	183	1.0	0.5	1.0	7.1×10^{-8}
glycerol-d_8	1058		0.6		4.1×10^{-7}

[a] Based on tables from the *Handbook of Chemistry* (Lange, 1961). [b] Correlation time obtained from Gly^6 methylene carbon T_1 value. [c] τ_0' values for glycerol/water mixtures are calculated as $\tau_0' = (\text{viscosity ratio})\tau_0(D_2O)$.

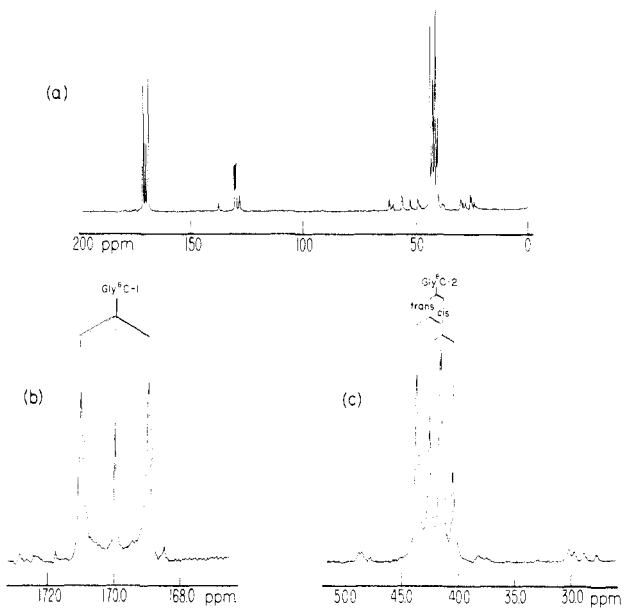

FIGURE 5: Proton-decoupled ^{13}C spectrum of [90%-1,2-$^{13}C_2$-Gly^6]-bradykinin: (a) full spectrum; (b) carbonyl resonances; (c) methylene resonances. The unusual peak shape of the carbonyl satellites arises as a consequence of the short T_1 of the coupled methylene carbon, as discussed in the text.

Solving for the intensity spectrum as described by Abragam gives

$$I(\omega) = \frac{1}{[J^2/4 - (\omega_0 - \omega)^2]^2 + [(\omega_0 - \omega)/T_1^M]^2} \quad (13)$$

where T_1^M is the spin–lattice relaxation time for spin M and J is the coupling constant in radians per second, i.e., $2\pi J$ (Hz). This result is analogous to that given by Gutowsky et al. (1953) with $T_2 \rightarrow \infty$ and with $\tau = 2T_1^M$, as well as to the absorption spectrum calculated for the case of chemical exchange leading to collapse of a doublet. Conversely, the effect of other broadening mechanisms which can contribute to T_2 can be included as described by Gutowsky et al. by setting $\tau = 2T_1^M$ in their treatment. It can be seen from the above expression that in many cases the T_1 values for protonated carbons in reasonably large biological molecules, i.e., $M_r > 1000$, will be sufficiently short to lead to broadening of the resonances of nuclei, e.g., ^1H or ^{13}C, to which they are scalar coupled. In this relatively slow relaxation limit, the incremental broadening for the ^{13}C A resonance will be given by

$$\Delta\nu^A = \frac{1}{2\pi T_1^M} \quad (14)$$

Results and Discussion

The proton-decoupled spectrum of [90%-1,2-$^{13}C_2$-Gly^6]-bradykinin (sequence Arg^1-Pro^2-Pro^3-Gly^4-Phe^5-Gly^6-Pro^7-Phe^8-Arg^9) obtained in D_2O is shown in Figure 5. As discussed previously (London et al., 1979), the cis/trans equilibrium results in additional splitting of the resonances of the Gly^6 methylene carbon but not of the Gly^6 carbonyl for which δ(cis–trans) = 0. From the spectrum, $^1J_{CC}$ values of 52.4 and 52.0 Hz corresponding to the trans and cis peptide conformations are obtained. As a result of the 1.1-ppm shift difference for the Gly^6 methylene between cis and trans conformers (London et al., 1979), the center resonance of the cis overlaps the upfield doublet of the trans, and the downfield cis doublet resonance overlaps the center trans resonance. An inversion–recovery experiment for the carbonyl resonance clearly indicated the more rapid relaxation of the ^{13}C–^{13}C doublet resonances resulting from the additional dipolar interaction (Figure 6). As is apparent from Figure 1, in the extreme narrowing region the relaxation of the carbons is exponential and described by g_A (eq 2), corresponding to a sum of the dipolar interactions with the other carbon and the protons. In this motional limit, a rotational correlation time τ_{cc} may be obtained based on the difference between the two curves:

$$\frac{1}{T_1}(\text{satellite}) - \frac{1}{T_1}(\text{center}) = \frac{\gamma_c^4\hbar^2}{10r_{cc}^6}\left[\frac{\tau_{cc}}{1 + (\omega_c - \omega_c')^2\tau_{cc}^2} + \frac{3\tau_{cc}}{1 + \omega_c^2\tau_{cc}^2} + \frac{6\tau_{cc}}{1 + (\omega_c + \omega_c')^2\tau_{cc}^2}\right] \quad (15)$$

Unfortunately, in the D_2O solvent, overlap of the carbonyl resonances corresponding to the cis and trans peptides precludes a determination of motional differences. Previous measurements of [20%-1,2-$^{13}C_2$-Gly^6]bradykinin in methanol/water mixtures have indicated a significant difference in the relaxation behavior of the cis and trans peptides monitored by the Gly^6 methylene resonances (London et al., 1979). In the D_2O solvent, no observable difference for the methylene cis and trans relaxation rates was noted. A rotational correlation time was also determined on the basis of the Gly^6 methylene carbon T_1 values and is included in Table I. It is interesting to note that the latter is significantly shorter than the τ_{cc} value calculated as described above.

A review of the minimal literature currently available for ^{13}C-enriched systems indicates that the discrepancy between the τ_{CC} and τ_{CH} values determined on the basis of nonprotonated carbon T_1 difference measurement as above and the adjacent protonated carbon T_1 values, respectively, is obtained in all cases (Table II). In our previous study of 6-phosphogluconate, this discrepancy was ascribed to anisotropic motion. Similarly, internal motion about the carbon–carbon bond will leave the ^{13}C–^{13}C dipolar interaction unchanged, while leading to a shorter rotational correlation time for the ^{13}C–^1H interactions. This effect can be readily observed in [1,2-$^{13}C_2$]acetate (Suzuki et al., 1975). The recent suggestions that the appropriate C–H bond length may be greater than 1.09 Å provide an alternative explanation for these dis-

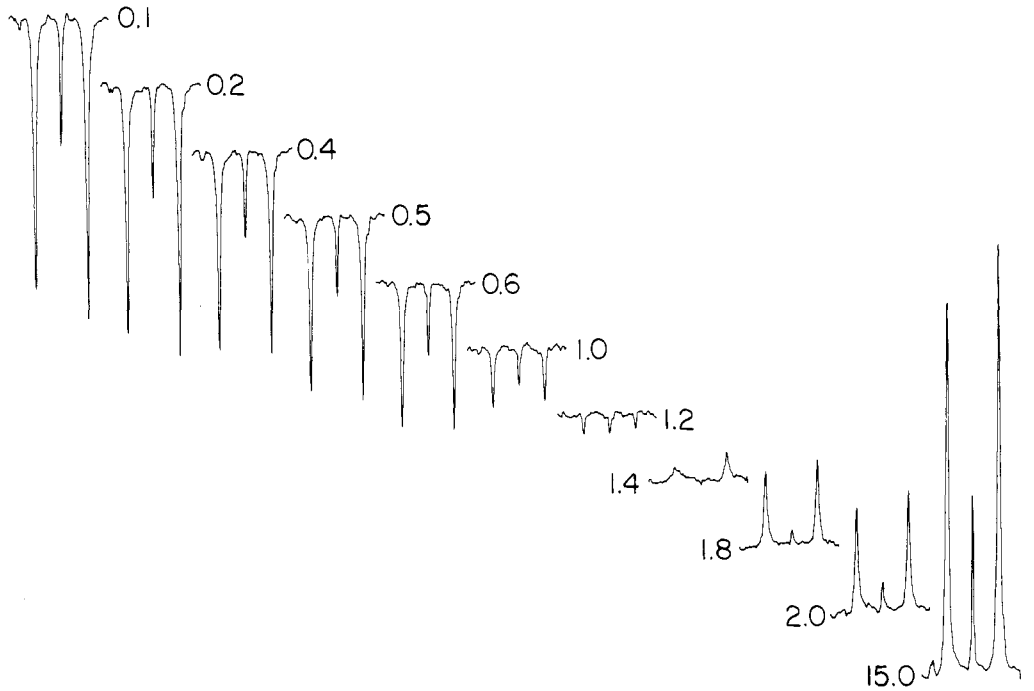

FIGURE 6: Inversion–recovery study of the carbonyl resonances of [90%-1,2-$^{13}C_2$-Gly^6]bradykinin. The additional contribution of the carbon–carbon dipolar interaction is most apparent for the delay of 1.4 s.

Table II: Rotational Correlation Times (s) for ^{13}C-Enriched Molecules

molecule	T_1^{CC}	$N_H T_1^{CH}$	τ_{CC}	τ_{CH}	ratio
diethylmalonate[a]	263	5.40	2.1×10^{-11}	8.6×10^{-12}	2.5
6-phosphogluconate[b]	53.5	0.765	1.05×10^{-10}	6.1×10^{-11}	1.7
[85%-1,2-$^{13}C_2$,97%-2,2-$^2H_2$] glycine[c]	*d*	41.0	1.7×10^{-11}	5.5×10^{-12}	3.1
[90%-1,2-$^{13}C_2$-Gly^6] bradykinin	14.3	0.20	3.9×10^{-10}	2.3×10^{-11}	1.7

[a] Data from Moreland & Carroll (1974). [b] Data from London et al. (1975b). [c] Data from Nery & Canet (1981). [d] Relaxation is non-exponential.

crepancies (Dill & Allerhand, 1979). However, an increase in bond length to 1.11 Å, as used recently by Dill and Allerhand, leading to a 12% increase in the calculated rotational correlation time will be insufficient to explain the observed effects. Additional studies of molecules for which anisotropic motion is expected to affect the carbon–carbon and carbon–proton interactions similarly, so that no effective correlation time differences for the two interactions exist, are currently in progress.

A significant difference between the line widths of the satellite and center resonances corresponding to the Gly^6 carbonyl is also observed (Figure 5b, Table III). The magnitude of this effect cannot be explained on the basis of the cis/trans equilibrium, since the coupling constants differ by only 0.4 Hz. The observed line-width difference presumably reflects a contribution arising from the short methylene T_1 as discussed in the previous section. Support for this interpretation also comes from a consideration of the peak shapes which indicate significant skewing of intensity toward the center of the pattern. The observed line-width values of 1.3 and 3.6 Hz for the center and satellite resonances, respectively, imply a contribution of 2.3 Hz. A simulated spectrum corresponding to a T_1^M value of 0.1 s as observed (Figure 6) leads to a 1.6-Hz line-width contribution, in reasonable agreement with the observed values. On the basis of eq 14, the 2.3-Hz line-width difference would correspond to $T_1^M \simeq 70$ ms. The discrepancy in this case may result from additional broadening, reflecting the cis/trans isomerism.

In order to study the effect of the ^{13}C–^{13}C dipolar interaction on ^{13}C relaxation for slower motion, i.e., in a motional region

Table III: Carbonyl Line Widths for [90%-1,2-$^{13}C_2$-Gly^6] Bradykinin

solvent	$\nu_{1/2}$ (center) (Hz)	$\nu_{1/2}$ (satellites) (Hz) downfield	$\nu_{1/2}$ (satellites) (Hz) upfield	$\Delta\nu^a$ (Hz)	T_1^M (ms)
D_2O	1.3	3.6	3.7	2.3	70
30% D_2O/70% glycerol-d_8	2.7	6.7	7.4	4.0	40
20% D_2O/80% glycerol-d_8	4.9	9.5	10.3	4.6	32
10% D_2O/90% glycerol-d_8	9.8	11.3	15.4	1.5	45
glycerol-d_8	*b*	25.4			

[a] Line-width difference defined as $\nu_{1/2}$(average) – $\nu_{1/2}$(center); the upfield/downfield line-width difference presumably reflects the cross-correlation between the ^{13}C–^{13}C dipolar and chemical shift anisotropy terms (Shimizu, 1964; L. G. Werbelow, private communication). [b] At high viscosities, ^{13}C–^{13}C dipolar broadening may contribute significantly to the satellite line widths so the interpretation in terms of T_1^M becomes more approximate (see Figure 3).

analogous to that characterizing small proteins, measurements were made at high viscosities corresponding to glycerol/water solutions. Previous studies of gramicidin S in solvents of varying viscosity have obtained rotational correlation times for the backbone resonances proportional to the viscosity as predicted on the basis of the Stokes–Einstein relation (Allerhand & Komoroski, 1973; Komoroski et al., 1975; Bothner-By & Johner, 1978). Since the peptide under study here is noncyclic, and since the microviscosity factor (Deslauriers

& Smith, 1977) may not remain unchanged for the very large viscosity changes involved in the present study, generalization to the present case may not be warranted. Rotational correlation times estimated from the value determined in D_2O and the viscosity ratio obtained from Lange (1961) are included in Table I.

Measurement of the carbonyl T_1 values in 30% D_2O/70% glycerol-d_8 (Table I) indicates that the ^{13}C–^{13}C dipolar interaction contributes a relatively larger fraction than in D_2O. The calculated T_1 contribution of 2.3 s is in excellent agreement with the value of 2.4 s estimated by using the calculated rotational correlation time of 7.8×10^{-9} s and the data in Figure 1b. Since this correlation time is close to the T_1 minimum, the broadening effect on the carbonyl doublet resonances due to the short methylene T_1 should be maximal. Analysis of the line-width data by using eq 14 leads to a T_1^M of 40 ms, in fair agreement with a predicted value of 24 ms from Figure 1b.

The basis for the small discrepancies encountered above becomes more clear by considering data obtained at higher glycerol/water ratios. In particular, it is apparent that the ^{13}C T_1 value for the center carbonyl resonance of 1.0 s determined in 10% D_2O/90% glycerol-d_8 is grossly inconsistent with the value expected on the basis of Figure 1b by using a rotational correlation time of 7.1×10^{-8} s. The explanation for this apparent inconsistency is straightforward: The peptide does not behave as a rigid isotropic rotor. At high viscosities, the T_1 values are dominated by internal segmental motions. The effect of segmental motion on peptide relaxation behavior is generally difficult to interpret [London (1980) and references cited therein]. This reflects in part the fact that the spin–lattice relaxation is determined primarily by motion closest to the T_1 minimum. For typical length peptides, the overall diffusion rate is fairly close to the T_1 minimum. In high-viscosity solvents, this is no longer the case, and segmental motions with rates close to the T_1 minimum will thus become "unmasked", at least from the standpoint of the T_1 measurement.

Several dynamic models can be applied to describe the segmental motion in peptides. Perhaps the simplest is the imposition of a conic boundary condition which has been treated by several groups (Bull et al., 1978; Howarth, 1979; Richarz et al., 1980; Wang & Pecora, 1980). All of these models give qualitatively similar results; e.g., using the model of Richarz et al. leads to a spectral density of the following form:

$$J(\omega) = C\frac{\tau_0}{1 + \omega^2\tau_0^2} + (1 - C)\frac{\tau'}{1 + \omega^2\tau'^2} \qquad (16)$$

where

$$C = \tfrac{1}{4}\cos^2\theta_{max}(1 + \cos\theta_{max})^2$$

for $0° \leq \theta_{max} < 70°$ and

$$\frac{1}{\tau} = \frac{1}{\tau_0} + \frac{3.45}{\tau_i \sin^2\theta_{max}}$$

In the above relations, θ_{max} defines the limit of the cone, τ_0 is the isotropic rotational correlation time of the axis of the cone, and τ_i is the correlation time for internal motion bounded by the surface of the cone. Since this type of motion affects all internuclear dipolar interactions similarly, each term in eq 2 and 3 of the form $\tau/(1 + \omega^2\tau^2)$ is replaced by a term of the form of eq 16. Calculations analogous to those presented in Figure 1 utilizing the above model have been carried out. These calculations predict the important qualitative features noted above; in particular, for internal motion with a range $\theta_{max} \sim 30°$ and a segmental motion rate close to the T_1 minimum, the observed T_1 values will increase more slowly for long correlation times than in the absence of segmental motion. In addition, the methylene T_1 value becomes slightly longer, in better agreement with the values predicted from the carbonyl line-width differences.

A quantitative approach to the data was attempted by (1) using the values in Table I for τ_0, (2) using the carbonyl line widths to determine the value of θ_{max} since this parameter is relatively insensitive to the value of τ_i, and (3) using the T_1 data to determine τ_i after the other two parameters are set. Unfortunately, the line-width data summarized in Table III are not suitable for this approach. These data imply dipolar broadening contributions which are larger than would be predicted by using the correlation times in Table I and setting $\theta_{max} = 0°$. It is generally well established that peptides in solution adopt a distribution of rapidly interconverting conformations. In the high-viscosity solvents, the rates of these interconversions may be substantially reduced, leading to additional broadening. Further, these conformations may also be characterized by different coupling constants. There is also a marked line-width asymmetry between the upfield and downfield doublets, as reflected in Table III. This may also be related to the conformational distribution characterizing the peptides or to cross-correlation effects involving the ^{13}C–^{13}C dipolar and chemical shift anisotropy terms (Shimizu, 1964). For these reasons, there seems to be little basis for attempting a more quantitative interpretation of the data at very high viscosities.

Conclusions

Several interesting conclusions follow from the present study: (1) A consistent difference is obtained for the rotational correlation time deduced on the basis of the ^{13}C–^{13}C dipolar interaction evaluated from the difference in relaxation behavior between the satellite and center ^{13}C resonances, and the correlation time obtained on the basis of the T_1 of protonated carbons. This discrepancy can be explained on the basis of motional anisotropy; however, additional work with small, rigid molecules is required to further investigate this effect. (2) In studies where relatively large molecules with long rotational correlation times are to be investigated, and where the doublet resulting from scalar ^{13}C–^{13}C coupling does not lead to unacceptable spectral complexity, multiple ^{13}C enrichment may be an effective tool for reducing the spin–lattice relaxation time, leading to very significant gains in sensitivity. (3) For particular rotational correlation times determined by the magnetic field strength at which the experiment is done, the ^{13}C–^{13}C dipolar interaction can significantly perturb the relaxation behavior of *protonated* carbons, leading to a nonexponential recovery. At 2.35 T, this effect is most pronounced for rotational correlation times near 10^{-7} s. At higher field, this effect corresponds to shorter correlation times, i.e., to values more typical of small proteins. (4) Broadening of ^{13}C–^{13}C multiplets due to short T_1 values for immobilized carbons with correlation times close to the T_1 minimum may prove useful for obtaining T_1 information. This effect may in some cases collapse small long-range couplings.

Acknowledgments

Stimulating discussions with E. Fukushima and with L. G. Werbelow of the New Mexico Institute of Mining and Technology were of much value in the development of this work.

References

Abragam, A. (1961) *The Principles of Nuclear Magnetism*, Clarendon Press, Oxford.

Allerhand, A. (1978) *Acc. Chem. Res. 11*, 469.
Allerhand, A., & Komoroski, R. A. (1973) *J. Am. Chem. Soc. 95*, 8228.
Allerhand, A., Doddrell, D., & Komoroski, R. A. (1971) *J. Chem. Phys. 55*, 189.
Bothner-By, A. A., & Johner, P. E. (1978) *Biophys. J. 24*, 779.
Bull, T. E., Norne, J. E., Reimarsson, P., & Lindman, B. (1978) *J. Am. Chem. Soc. 100*, 4643.
Canet, D., Nery, H., & Brondeau, J. (1979) *J. Chem. Phys. 70*, 2098.
Deslauriers, R., & Smith, I. C. P. (1977) *Biopolymers 16*, 1245.
Dill, K., & Allerhand, A. (1979) *J. Am. Chem. Soc. 101*, 4376.
Gupta, R. K. (1977) *J. Magn. Reson. 25*, 231.
Gutowsky, H. S., McCall, D. W., & Slichter, C. P. (1953) *J. Chem. Phys. 21*, 279.
Howarth, O. W. (1979) *J. Chem. Soc., Faraday Trans. 2 75*, 863.
Jeffers, P. K., Sutherland, W. M., & Khalifah, R. G. (1978) *Biochemistry 17*, 1305.
Komoroski, R. A., Peat, I. R., & Levy, G. C. (1975) *Biochem. Biophys. Res. Commun. 65*, 272.
Lange, N. A. (1961) *Handbook of Chemistry*, McGraw-Hill, New York.
London, R. E. (1980) in *Magnetic Resonance in Biology* (Cohen, J. S., Ed.) p 1–69, Wiley-Interscience, New York.
London, R. E., & Avitabile, J. (1976) *J. Chem. Phys. 65*, 2443.
London, R. E., Matwiyoff, N. A., Kollman, V. H., & Mueller, D. D. (1975a) *J. Magn. Reson. 18*, 555.
London, R. E., Matwiyoff, N. A., & Mueller, D. D. (1975b) *J. Chem. Phys. 63*, 4442.
London, R. E., Stewart, J. M., Williams, R., Cann, J. R., & Matwiyoff, N. A. (1979) *J. Am. Chem. Soc. 101*, 2455.
Moreland, C. G., & Carroll, F. E. (1974) *J. Magn. Reson. 15*, 596.
Nery, H., & Canet, D. (1981) *J. Magn. Reson. 42*, 370.
Norton, R. S., & Allerhand, A. (1976) *J. Am. Chem. Soc. 98*, 1007.
Pople, J. A. (1958) *Mol. Phys. 1*, 168.
Richarz, R., Nagayama, K., & Wuthrich, K. (1980) *Biochemistry 19*, 5189.
Schaublin, S., Hohener, H., & Ernst, R. R. (1974) *J. Magn. Reson. 13*, 196.
Shimizu, H. (1964) *J. Chem. Phys. 40*, 3357.
Suzuki, K. T., Cary, L. W., & Kuhlmann, K. F. (1975) *J. Magn. Reson. 18*, 390.
Virlet, J., & Ghesquieres, D. (1980) *Chem. Phys. Lett. 73*, 323.
Wang, C. C., & Pecora, R. (1980) *J. Chem. Phys. 72*, 5333.

The Protein Synthesis Inhibitor Thermorubin. 1. Nature of the Thermorubin–Ribosome Complex†

Fwu-lai Lin‡ and Arnold Wishnia*

ABSTRACT: Thermorubin behaves as a triprotic acid, TrH_3, with pK_as of 4.7, 7.1, and 9.1 (22 °C, 10% v/v aqueous ethanol, corrected to zero ionic strength). Mg^{2+} successively forms TrH·Mg and $Tr{\cdot}Mg_2^+$ complexes with formation constants $L_{11} = [TrH{\cdot}Mg]/([Mg^{2+}][TrH^{2-}]) = 3.3 \times 10^4\ M^{-1}$ and $L_{12H} = [Tr{\cdot}Mg_2^+][H^+]/([TrH{\cdot}Mg][Mg^{2+}]) = 1.4 \times 10^{-5}$. The first proposed structure (I) [Moppett, E., Dix, D. T., Johnson, F., & Coronelli, C. (1972) *J. Am. Chem. Soc. 94*, 3269–3272] is incompatible with these results. The pK_a's of TrH_3 are compatible with ionization of the carboxylic acid, the enolic β-diketone, and one of the phenolic groups of the new structure (II) [Johnson, F., Chandra, B., Iden, C. R., Naiksatam, P., Kahen, R., Okaya, Y., & Lin, S.-Y. (1980) *J. Am. Chem. Soc. 102*, 5580–5585]. Plausible structures for TrH·Mg and $Tr{\cdot}Mg_2^+$ can be suggested. All species have absorbance maxima near 300, 330, and 430 nm, with absorptivities of 30–60, 20–50, and 15–20 $mM^{-1}\ cm^{-1}$, respectively. TrH_n and TrH·Mg have broad featureless emission spectra, maximal at 585 nm, with quantum yields of about 0.004 and 0.010. $Tr{\cdot}Mg_2^+$ is not fluorescent. TrH·Mg and $Tr{\cdot}Mg_2^+$ are the predominant species at intracellular ionic concentrations. Centrifuge and fluorescence enhancement studies show that *Escherichia coli* 70S ribosomes and 30S and 50S subunits all have a single site for binding thermorubin, with $K_D = 1.9 \times 10^{-8}$, 1.9×10^{-6}, and 1.4×10^{-6} M (25 °C, 10 mM Mg^{2+}, 60 mM M^+, pH 7.5). Thermorubin binds to ribosomes more strongly than streptomycin and binds orders of magnitude more strongly than the structurally comparable tetracyclines. The limiting fluorescence enhancements, $E_\infty = (F_{bound,molar}/F_{free,molar}) - 1$, are 0.54, 1.41, and 1.53 (for 70 S, 30 S, and 50 S, respectively). Iodide ion quenching of free Tr, 30 S·Tr, and 50 S·Tr follows the same Stern–Volmer curve, while 70 S·Tr fluorescence is not quenched at all: the thermorubin binding sites must lie on the surfaces of the 30S and 50S subunits and inside the 70S particles. It is not improbable that the weaker subunit sites are corresponding portions of the strong 70S site. It is very likely that the actual inhibitory species is the neutral fluorescent TrH·Mg complex.

The antibiotic thermorubin, discovered in 1964 (Craveri et al., 1964), was later shown to inhibit protein synthesis, but not DNA and RNA synthesis, in *Escherichia coli* in vivo and to inhibit initiator tRNA binding to ribosomes in vitro (Pirali et al., 1974). Our concern in this paper is the identity of the effective species among the set at equilibrium in physiological ionic solutions and the elementary characterization of its target: the number, location, and affinity of the principal ribosomal binding site(s). The unusual, perhaps unique, mode of action of thermorubin is described in the following paper (Lin & Wishnia, 1982).

† From the Department of Chemistry, State University of New York at Stony Brook, Stony Brook, New York 11794. *Received June 5, 1981; revised manuscript received September 21, 1981.* Taken, in part, from the thesis of F.-l.L., submitted in partial fulfillment of the requirements for Ph.D., State University of New York at Stony Brook. Supported in part by National Institutes of Health Grant GM27176.

‡ Present address: Cancer Biology Program, Frederick Cancer Research Center, National Cancer Institute, Frederick, MD 21701.

0006-2960/82/0421-0477$01.25/0